Journal of Materials Chemistry

Accepted Manuscript

RSC Publishing

www.rsc.org/materials
Registered Charity Number 207890

Sponge-like porous carbon/tin composite anode materials for lithium ion batteries

Yunhua Xu, Juchen Guo and Chunsheng Wang*

Department of Chemical and Biomolecular Engineering, University of Maryland, College Park, MD 20742, USA
E-mail: cswang@umd.edu

Keywords: tin, porous carbon, anode, lithium-ion battery

A novel sponge-like porous C/Sn composite is synthesized by dispersing SnO_2 nanoparticles into soft-template polymer matrix followed by carbonization. The mesoporous C/Sn anodes can deliver a capacity of as high as 1300 mAh/g after 450 charge/discharge cycles, and provide capacity of 180 mAh/g even at 4000 mA/g charge/discharge current density. An extra reversible capacity over the theoretical value of the porous C/Sn anode is observed, which is attributed to the reversible formation/decomposition of gel-like polymers formed on the mesoporous C/Sn composite due to the catalytic effect of Sn nanoparticles. The high capacity, long cycle life, high power, ~100% coulombic efficiency, and inexpensive production method make the sponge-like porous C/Sn composite an attractive anode material in Li-ion batteries for electric vehicles and renewable energy storage.

Introduction

Developing rechargeable batteries with high capacity, high rate capability, and long cycling life is the key to the success of electric vehicles (EV) and the use of renewable energies, such as wind and solar energies. Lithium ion batteries, the most popular power sources on markets for portable electronic devices, can be used for EV if the energy density can be enhanced.[1] In the last decade, extensive efforts have been made to increase the capacity of anodes by replacing currently used graphite with Si or Sn.[2-5] Although Si has higher gravimetric capacity (3572 mAh/g) than that of Sn (992 mAh/g), their volumetric capacities are similar (8322 mAh/cm^3 for Si and 7254 mAh/cm^3 for Sn), and both are considerably larger than that of graphite (818 mAh/cm^3). The volumetric energy density is the most relevant metric for most Li-ion battery applications.[6] However, practical application of Sn anodes is hampered by the poor cycling stability due to large volume change of 260% as well as aggregation during lithiation/delithiation processes.[7-15] The strain-induced pulverization would lead to loss contact to current collector, resulting a fast capacity fading.

The most successful method for improving the cycling stability is to form a C/Sn nanocomposite.[13-15] Electro-spin has been used to synthesize C/Sn composite by dispersing Sn nanoparticles in porous multichannel carbon microtubes[10] or bamboo-like hollow carbon nanofibers[11]. The porous C/Sn composite materials have two fold advantages: (1) the porous structure of C/Sn composites provides additional space to accommodate the volume variation reducing the tin particle pulverization; (2) the porous carbon matrix can avoid oxidation and aggregation of Sn nanoparticles and provides continuous electron pathway. However, the electro-spin synthesis approach still faces challenges to control the morphology and component ratio of C/Sn. Therefore, a simple route for synthesis of porous C/Sn composite anode materials is highly desired, especially for transforming research efforts into commercial products.

In this paper, a novel sponge-like mesoporous C/Sn composite was prepared using soft-template method[17-19] by carbonizing phase-separated polymer/SnO_2 nanoparticle composite precursor. SnO_2 nanoparticles were reduced to Sn nanoparticles under presence of carbon during the carbonization process. Resorcinol-formaldehyde (RF) was used as the carbon source, and triblock copolymer of poly(ethylene oxide)-*b*-poly(propylene oxide)-*b*-poly(ethylene oxide) (EO_{106}-PO_{70}-EO_{106}, Pluronic F127) was used as the sacrificial template to form pores in carbon. The interaction between these two polymers promoted self-assembled nanostructure through phase-separation. The template block copolymer decomposed in the subsequent carbonization to form pores, and the RF polymer framework was carbonized as carbon walls. The resulting porous carbon exhibited large pore volume and thin carbon walls, making it like carbon sponge. Tin nanoparticles were well dispersed in this unique porous structure that can accommodate the large volume change during charge/discharge cycling. The resiliency and conductivity of carbon walls could provide mechanical support to alleviate tin particle pulverization and ensure good electric contact.[13,14,20,21] The aggregation of tin particles could also be prevented by the carbon sponge.[9,12] With these features, high specific capacity and long cycling life are expected from this porous C/Sn nanoparticle composite anode material for lithium ion batteries.

Experimental

Synthesis of Porous Carbon/Tin Nanoparticle Composite

The synthesis of porous C/Sn composite materials consisted of three steps: preparation of polymer solution, SnO_2 nanoparticle dispersion, and carbonization. All materials were purchased from Sigma-Aldrich and were used without further purification. The polymer solution was prepared by dissolving 0.33 g resorcinol (R), 0.22 g triblock copolymer (Pluronic F127) and 1 ml 1% NaOH aqueous solution in 5 ml *N,N*-dimethylformamide (DMF), where the triblock copolymer and the NaOH functioned as soft-template and catalyst,

respectively. When the solution was clear, 0.4 g 37% formaldehyde (F) aqueous solution was added. After 30 min vigorous stirring, the solution was stirred for another 30 min at 80ºC to promote the polymerization reaction between resorcinol and formaldehyde. In the meanwhile, 0.5 g SnO_2 nanoparticles (<100 nm) were dispersed into 30 ml DMF by ultrasonication. Then the obtained solution was added into the dispersion and underwent ultrasonic treatment. The mixture was dried while stirring at 100°C overnight and further cured in an oven at 100°C for 24 h. Finally, the polymer/SnO_2 composite was carbonized with heating ramp of 2°C/min in flowing argon at 400°C for 3 h and then 700°C for additional 3 h. For comparison, porous carbon without Sn was synthesized using the same procedure described above.

Material Characterizations

Scanning electron microscopy (SEM) and transmission electron microscopy (TEM) images were taken by Hitachi SU-70 analytical ultra-high resolution SEM (Japan) and JEOL (Japan) 2100F field emission TEM, respectively. X-ray diffraction (XRD) pattern was recorded by Bruker Smart1000 (Bruker AXS Inc., USA) using CuKα radiation. Thermogravimetric analysis (TGA) was carried out using thermogravimetric analyzer (TA Instruments, USA) with a heating rate of 10°C/min in air. BET specific surface area and pore size and volume were analyzed using N_2 absorption on TriStar 3020 (Micromeritics Instrument Corp., USA).

Electrochemical Measurements

The porous C/Sn composite was mixed with carbon black and sodium carboxymethyl cellulose (CMC) binder to form a slurry at the weight ratio of 70:15:15. The electrode was prepared by casting the slurry onto copper foil using a doctor blade and dried in a vacuum oven at 100°C overnight. Coin cells were assembled with lithium foil as the counter electrode, 1M $LiPF_6$ in a mixture of ethylene carbonate/diethyl carbonate (EC/DEC, 1:1 by volume) as the electrolyte, and Celgard®3501 (Celgard, LLC Corp., USA) as the separator. Cells with

pure porous carbon electrodes were also fabricated using the same procedure. Electrochemical performance was tested using Arbin battery test station (BT2000, Arbin Instruments, USA). Capacity was calculated on the basis of the total mass of the porous C/Sn composite. Cyclic voltammogram scanned at 0.2 mV/s between 0 – 3 V was recorded using Solatron 1260/1287 Electrochemical Interface (Solartron Metrology, UK).

Results and Discussion

Structure of porous C/Sn composite

Fig. 1a shows the SEM image of the porous C/Sn composite. It is clearly seen that tin nanoparticles with particle size of around 100 nm are uniformly embedded in a sponge-like porous carbon matrix. Pores with diameter of around 10 nm are separated by very thin carbon walls. The unique sponge-like carbon matrix will provide large void space and mechanical support to release strain induced by the alloying/dealloying of tin, thus preventing pulverization of tin particles.

Sn particle size and distribution in the carbon sponge was also investigated using TEM, shown in Fig. 1b and c. Sn nanoparticles with an average particle diameter of about 100 nm were uniformly dispersed in porous carbon matrix, which is consistent with SEM results. The particle size is similar to that of SnO_2 nanoparticles which were used as the tin source, demonstrating that the Sn nanoparticles were well dispersed and confined in the carbon matrix, and no aggregation occurred even when Sn became liquid during carbonization at a temperature higher than the melting point of tin metal. These results suggested that the sponge-like carbon matrix may prevent the aggregation of tin particles during prolonged cycling, improving cycling stability. High-resolution transmission electron microscopy (HRTEM) and selected area electron diffraction (SAED) images (Fig. 1c and insert) revealed that Sn nanoparticle is in crystalline structure, which was also confirmed by X-ray diffraction

(XRD) pattern (Fig. 2). All the peaks in Fig. 2 could be indexed to crystal tin (JPCDS card No. 86-2264). No peaks attributed to SnO_2 were detected, indicating that the SnO_2 particles were completely converted to crystal tin.

The porous structure of the C/Sn composite was characterized by N_2 adsorption measurement. Fig. 3 depicts the adsorption isotherm and the pore size distribution analyzed by Barrett−Joyner−Halenda (BJH) method. The Brunauer−Emmett−Teller (BET) specific surface area of the porous C/Sn composite is 180 m^2/g and the pore volume is 0.16 cm^3/g. BJH average pore diameter is 7 nm (Fig. 3b), which is in accordance with previous reports.[17,18] The large specific surface area and pore volume would benefit to alleviate strain, accommodate volume changes and improve the kinetics.

Composition and stability of porous C/Sn composite

Composition and thermal/chemical stability of the porous C/Sn composite were measured in air using TGA analysis (shown in Fig. 4). The small weight loss below 100°C in Fig. 4 was attributed to water evaporation. Almost no weight loss between 100°C to 220°C can be observed, demonstrating that both carbon and Sn in porous C/Sn composite are thermally and chemically stable in air up to 220°C, i.e. no Sn oxidation reaction and carbon decomposition occurred in air at 220°C. Therefore, the sponge-like mesoporous carbon/Sn composite prepared using soft-template method can be stored for a long-time without performance decline.[13,22] The weight gain from 220°C to 300°C is attributed to the oxidation of metallic tin ($Sn+O_2 \rightarrow SnO_2$), while the followed weight loss from 300°C to 480°C is mainly due to carbon decomposition ($C+O_2 \rightarrow CO_2$ (gas)).[13] The content of metallic tin in the composite was determined to be 66% using the following Equation 1:

$$Sn\ (wt\%) = 100 \times \frac{molecular\ weight\ of\ Sn}{molecular\ weight\ of\ SnO_2} \times \frac{final\ weight\ of\ SnO_2}{initial\ weight\ of\ C/Sn\ composite} \quad (1)$$

Electrochemical performance of porous C/Sn composite

Electrochemical behaviors of the porous C/Sn composite electrodes were investigated in coin-style half cells using lithium as the counter electrode. Fig. 5a shows the cyclic voltammograms of the initial 5 cycles. Two reduction peaks at 0.33 V and 0.6 V, are assigned to the lithiation reaction between tin and lithium to form Li_xSn alloy.[13,15,23] The corresponding oxidation peaks between 0.4 V and 0.8 V were assigned to the delithiation reaction of Li_xSn alloy.[13,15,23] The peak currents due to lithiation/delithiation of Sn were stabilized after initial small decline in the first three charge/discharge cycles. Two irreversible peaks at 1.05 V and 1.55 V, responsible for the catalytic decomposition of the electrolyte on tin, were not observed in the first lithiation. Therefore, it indicated that tin nano-particles were completely encapsulated in carbon matrix.[15] The reason for the abnormal peak near 3 V, which occurred only in the first oxidation scan and also reported on the C/Sn composite by other researchers,[24] was still not fully understood.

Fig. 5b illustrated the cycling stability of the porous C/Sn composite at the current density of 200 mA/g between 0.02 – 3 V. For comparison, the cycling behavior of porous carbon without tin nanoparticles was also evaluated in the same conditions. Theoretical capacity of the porous C/Sn composite (Sn:C=66:34 by weight), based on the theoretical capacity of metallic tin (992 mAh/g) and the actual capacity of pure porous carbon (335 mAh/g) in the first-cycle, was also shown in Fig. 5b. The capacity of porous C/Sn composite in the first delithiation was 769 mAh/g, which was closed to the theoretical capacity of the Sn and carbon composite (770 mAh/g). The specific capacity of the C/Sn composite gradually decreased to 620 mAh/g during the initial 30 charge/discharge cycles, and then began to increase and being stabilized at 1300 mAg/g after 300 cycles. Since the capacity of pure porous carbon continuously increased with charge/discharge cycles, the initial capacity decline of porous

C/Sn anodes should be attributed to slight degeneration of nano-Sn particles. The stabilized capacity of 1300 mAh/g after 300 cycles is much higher than that of current commercially used graphite and even higher than the theoretical capacity (770 mAh/g) of the composite. The similar capacity increasing behavior during charge/discharge cycles has also been reported on porous carbon,[25] SnO_2/graphene nanocomposite,[26] and Si/C nanocomposite anode materials[27] in lithium ion batteries. The mechanism behind is still not clear. Extra capacity over the theoretical capacity was also found in metal oxide anodes (such as CoO,[28,29] CuO,[30] and SnO_2, [24]), where the extra capacity was attributed to reversible formation of polymeric species at 0.8 V and dissolution above 2.1 V in alkyl carbonate solution due to the high catalytic activity of metal oxides nanoparticles.[28,29] The coulombic efficiency of porous C/Sn anodes increased quickly from initial 75% to almost 100% after 8 cycles. The porous C/Sn synthesized using simple carbonization technology showed higher capacity and longer cycling life than those C/Sn anodes reported in open literature.

To investigate the mechanism of the extra capacity in the porous C/Sn anode, the charge/discharge behaviors at different cycles were examined. Fig. 5c shows the charge/discharge behavior of the mesoporous Sn/Carbon composite anodes in the 1st, 30th, 60th, 100th, and 150th cycles. Since the lithiation curves of the mesoporous C/Sn was interfered by SEI formation during the initial few cycles, delithiation curves were examined for mechanism of the extra capacity. The first delithiation curve consists of three small plateaus at potential around 0.6-0.8V due to the formation of Li_xSn alloys, followed by a slop line due to lithiation of porous carbon. The decrease in delithiation capacity in the initial 30 cycles is mainly attributed to the reduced capacity of Li_xSn at plateau potential of 0.8 V, as evidenced by the parallel delithiation curves of the first and the 30th cycles above 0.8 V. During further cycles, the capacity of Li_xSn alloy was stable. However, the capacity above 1.2 V gradually increased. Here we attributed the increased capacity above 1.2 V to reversible decomposition

of gel-like polymer. The morphology of gel-like polymer on porous C/Sn anodes before decomposition was investigated using TEM after charging the electrode to 1V (Fig. 5d). A thick layer of gel-like polymer was clearly observed on the surface of the composite anode. The extra capacity over the theoretical capacity due to reversible formation of polymeric species at 0.8 V and dissolution above 2.1 V in alkyl carbonate solution was also found in metal oxide anodes (such as CoO,[28,29] CuO,[30] and SnO_2[24]). The decomposition potential (1.2 V) of the gel-like polymer on the porous C/Sn anode is much lower than those reported on CoO anodes (1.8 V).[28,29] This suggests that Sn has higher catalytic activity for the reversible formation/decomposition of gel-like polymer than the transition metals. The high catalytic role of Sn was also evidenced by the faster capacity increase in the mesoporous C/Sn than in the pure porous C anodes (Fig. 5b). It should be pointed out that the capacity delivered by the gel-like polymer on transition metal oxides anodes suffered a fast capacity fading after 100 cycles,[28,29] while the cycling stability of the mesoporous C/Sn composite was significantly improved, which was stabilized at 1300 mAh/g after 300 cycles.

If the delithiation capacity of porous C/Sn anodes at potential above 1.2 V is attributed to decomposition of gel-like polymer, the lithiation capacity due to formation of gel-like polymer in the following discharge should decrease when the charge cut-off potential decreases from 3 V to 1.5 V. To confirm this hypothesis, a porous C/Sn anode was firstly cycled at 200 mA/g between 0.02 V and 3 V for 97 cycles, and then was charged/discharged at the same current but in a narrower potential range between 0.02 V and 1.5 V for additional 103 cycles. Fig. 6a shows the capacity behavior of the porous C/Sn anodes in the total 200 charge/discharge cycles. The capacity retention during charge/discharge cycles is showed in Fig. 6a, and the corresponding charge/discharge curves using different cut-off potentials at the 97^{th}, 98^{th} and 200^{th} cycles were compared in Fig. 6b. As expected, the discharge capacity sharply decreased from 1040 mAh/g at the 97^{th} cycle to ~420 mAh/g at the 98^{th} cycle when

charge cut-off potential decreased from 3 V to 1.5 V (Fig. 6a). The capacity of porous C/Sn anodes should continually increase if the charge cut-off potential is still maintained at 3 V (Fig. 5b), but abruptly decline when the charge cut-off potential was decreased to 1.5 V. This is because the formed gel-like polymer in 97th discharge could not be decomposed at potential below 1.5 V in the 98th charge, so no new gel-like polymer could be formed in the following discharge, resulting in a decrease of the discharge capacity at the 98th cycle. Therefore, the reduced species could not be fully oxidized at a potential below 1.5 V, leading to that the extra capacity gradually vanished (Fig. 6b). The exact mechanism behind the extra capacity for mesoporous C/Sn anodes is still under investigation.

After the mesoporous Sn/carbon anodes were stabilized by charging/discharging for 100 cycles at 200 mA/g, the rate capability of the porous C/Sn composite was investigated at different currents. The excellent rate performance of porous C/Sn anodes was demonstrated in Fig. 7. A high capacity of 360 mAh/g was retained at the current density of 2000 mA/g, which is much higher than reported rate performance of C/Sn composite anodes using electrostatic spray deposition (ESD) technique.[31] Even at a higher current of 4000 mA/g, the capacity retention is still as high as 180 mAh/g. The enhanced rate capability is believed to be associated with the unique porous structure. The thin resilient carbon walls provide a mechanical support to enable good electric contact between tin particles and carbon matrix. In addition, the large specific surface area ensures a high electrode-electrolyte contact area, which could significantly improve the transport for electrons and lithium ions.

Conclusion

Sponge-like porous carbon/tin nanoparticle composite was synthesized by simply dispersing SnO_2 nanoparticles in polymer matrix and subsequent carbonization, where the self-assembled soft-template polymer decomposed during carbonization to form porous structure.

The porous Sn/C anodes can be charge/discharged for 450 cycles and maintain reversible capacity of 1300 mAh/g, which is much higher than the theoretical capacity of the mesoporous C/Sn composite. The extra capacity is attributed to the high catalytic activity of Sn for reversible formation/decomposition of gel-like polymer. The C/Sn anodes with unique porous structure also can deliver 360 mAh/g capacity even at 2000 mA/g charge/discharge current. In addition, the good thermal stability and simple synthesis make it very attractive as anode for lithium ion batteries, especially for commercial manufacture.

Acknowledgements

The authors gratefully acknowledge the support of the Army Research Office under Contract No.: W911NF1110231 (Dr. Robert Mantz, Program Manager) and Ellen Williams Distinguished Postdoctoral Fellowship.

References

1 U. Kasavajjula, C. S. Wang and A. J. Appleby, *J. Power Sources*, 2007, **163**, 1003.

2 J. W. Fergus, *J. Power Sources*, 2010, **195**, 939.

3 L. W. Ji, Z. Lin, M. Alcoutlabi and X. W. Zhang, *Energy. Environ. Sci.*, 2011, **4**, 2682.

4 Y. G. Guo, J. S. Hu and L. J. Wan. *Adv. Mater.*, 2008, **20**, 2878.

5 P. G. Bruce, B. Scrosati and J. M. Tarascon, *Angew. Chem. Int. Ed.*, 2008, **47**, 2930.

6 V. L. Chevrier and G. Ceder, *J. Electrochem. Soc.* 2011, **158**, A1011.

7 X. W. Lou, Y. Wang, C. L. Yuan, J. Y. Lee and L. A. Archer, *Adv. Mater.*, 2006, **18**, 2325.

8 Y. Wang, H. C. Zeng and J. Y. Lee, *Adv. Mater.*, 2006, **18**, 645.

9 G. Derrien, J. Hassoun, S. Panero and B. Scrosati, *Adv. Mater.*, 2007, **19**, 2336.

10 Y. Yu, L. Gu, C. B. Zhu, P. A. van Aken and J. Maier, *J. Am. Chem. Soc.*, 2009, **131**, 15984.

11 Y. Yu, L. Gu, C. L. Wang, A. Dhanabalan, P. A. van Aken and J. Maier, *Angew. Chem. Int. Ed.*, 2009, **48**, 6485.

12 I. S. Kim, G. E. Blomgren and P. N. Kumta, *Electrochem. Solid-State Lett.*, 2004, **7**, A44.

13 W. M. Zhang, J. S. Hu, Y. G. Guo, S. F. Zheng, L. S. Zhong, W. G. Song and L. J. Wan, *Adv. Mater.*, 2008, **20**, 1160.

14 K. T. Lee, Y. S. Jung and S. M. Oh, *J. Am. Chem. Soc.*, 2003, **125**, 5652.

15 Y. S. Jung, K. T. Lee, J. H. Ryr, D. Im and S. M. Oh, *J. Electrochem. Soc.*, 2005, **152**, A1452.

16 O. Mao, R. L. Turner, I. A. Courtney, B. D. Fredericksen and M. I. Buckett, *Electrochem. Solid-State Lett.*, 1999, **2**, 3.

17 Y. Meng, D. Gu, F. Zhang, Y. Shi, H. Yang, Z. Li, C. Yu, B. Tu and D. Y. Zhao, *Angew. Chem. Int. Ed.*, 2005, **44**, 7053.

18 S. Tanaka, N. Nishiyama, Y. Egashira and K. Ueyama, *Chem. Commun.* 2005, **2125**.

19 C. Liang and S. Dai, *J. Am. Chem. Soc.*, 2006, **128**, 5316.

20 J. C. Guo, X. L. Chen and C. S. Wang, *J. Mater. Chem.*, 2010, **20**, 5035.

21 J. C. Guo, A. Sun and C. S. Wang, *Electrochem. Commun.*, 2010, **12**, 981.

22 J. Hassoun, G. Derrien, S. Panero and B. Scrosati, *Adv. Mater.*, 2008, **20**, 3169.

23 D. Deng and J. Y. Lee, *Angew. Chem. Int. Ed.*, 2009, **48**, 1660.

24 B. Guo, J. Shu, K. Tang, Y. Bai, Z. Wang and L. Chen, *J. Power Sources*, 2008, **177**, 205.

25 S. Yang, X. Feng, L. Zhi, Q. Cao, J. Maier and K. Müllen, *Adv. Mater.*, 2010, **22**, 838.

26 P. Lian, X. Zhu, S. Liang, Z. Li, W. Yang and H. Wang, *Electrochim. Acta*, 2011, **56**, 4532.

27 A. Magasinski, P. Dixon, B. Hertzberg, A. Kvit, J. Ayala and G. Yushin, *Nat. Mater.*, 2010, **9**, 353.

28 S. Laruelle, S. Grugeon, P. Poizot, M. Dollé, L. Dupont and J-M. Tarasconz, *J. Electrochem. Soc.*, 2002, **149**, A627.

29 S. Grugeon, S. Laruelle, L. Dupont and J.-M. Tarascon, *Solid State Sci.*, 2008, **5**, 895.

30 A. Débart,z L. Dupont, P. Poizot, J-B. Leriche and J. M. Tarascon, *J. Electrochem. Soc.*, 2001, **148**, A1266.

31 X. Li , A. Dhanabalan and C. Wang, *Adv*. *Energ. Mater.*, DOI: 10.1002/aenm.201100380.

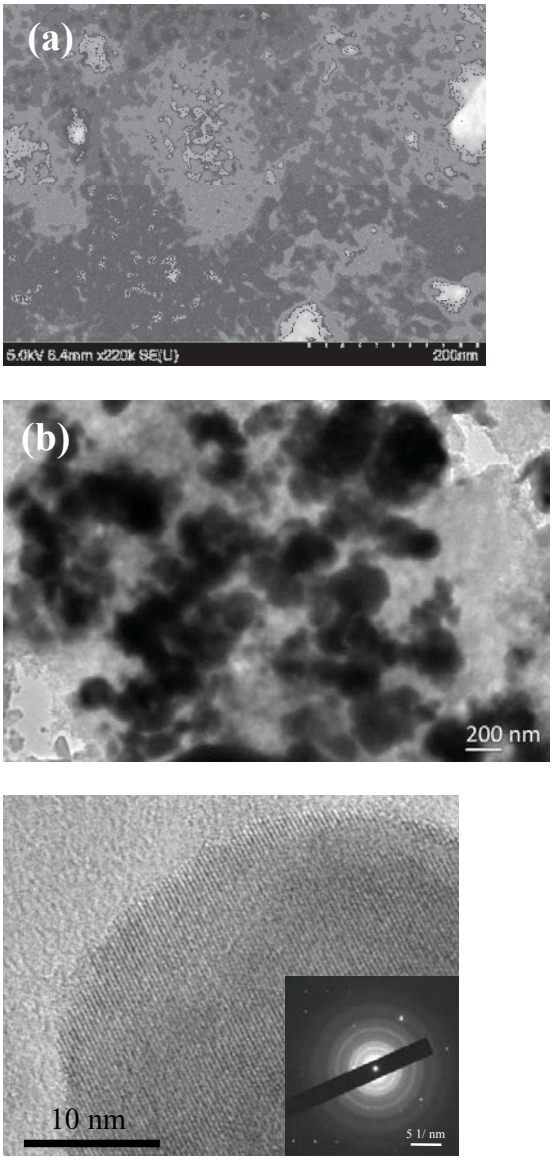

Fig. 1 (a) SEM, (b) TEM, and (c) HRTEM images of the porous C/Sn composite. Insert: SAED pattern of tin nanoparticles.

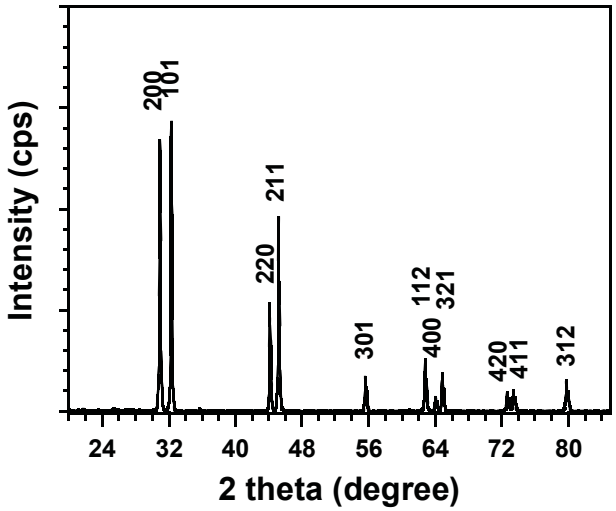

Fig. 2 XRD pattern of the porous C/Sn composite. The diffraction peaks for tin (card number) was indexed in XRD pattern.

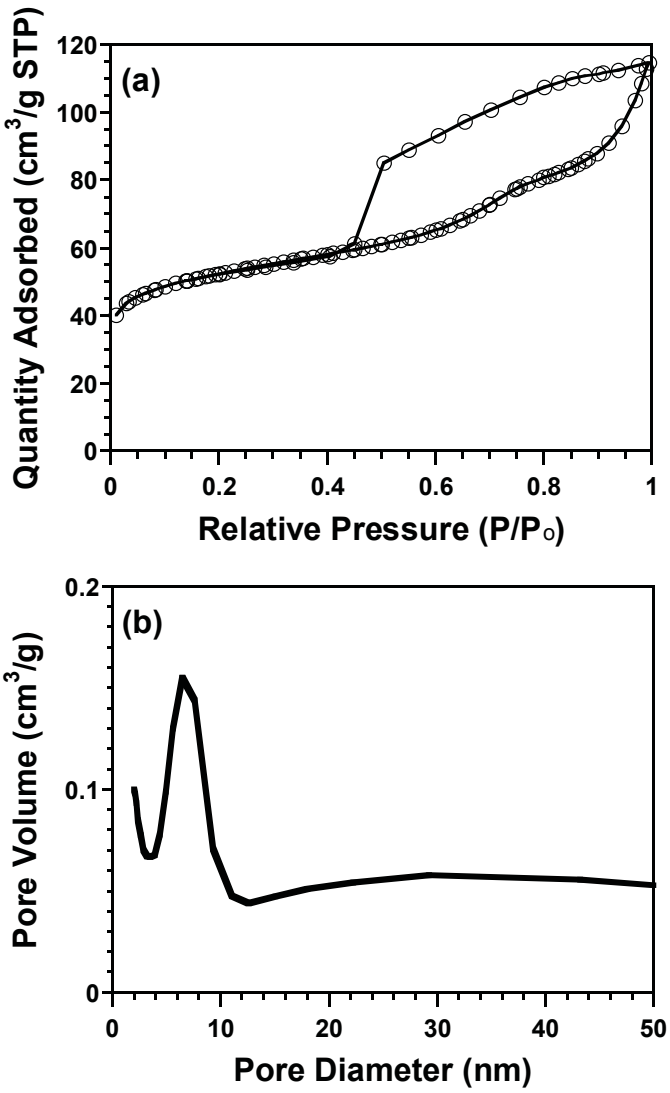

Fig. 3 (a) N_2 adsorption/desorption isotherm and (b) pore-size distribution curve of the porous C/Sn composite.

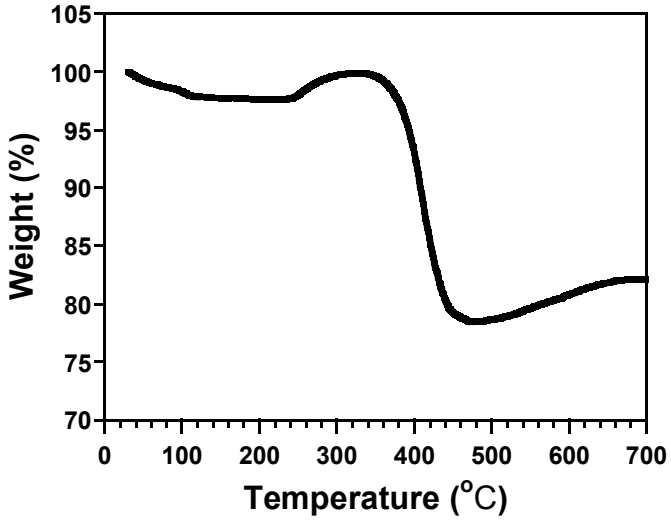

Fig. 4 Thermogravimetric (TGA) curve of porous C/Sn composite in air.

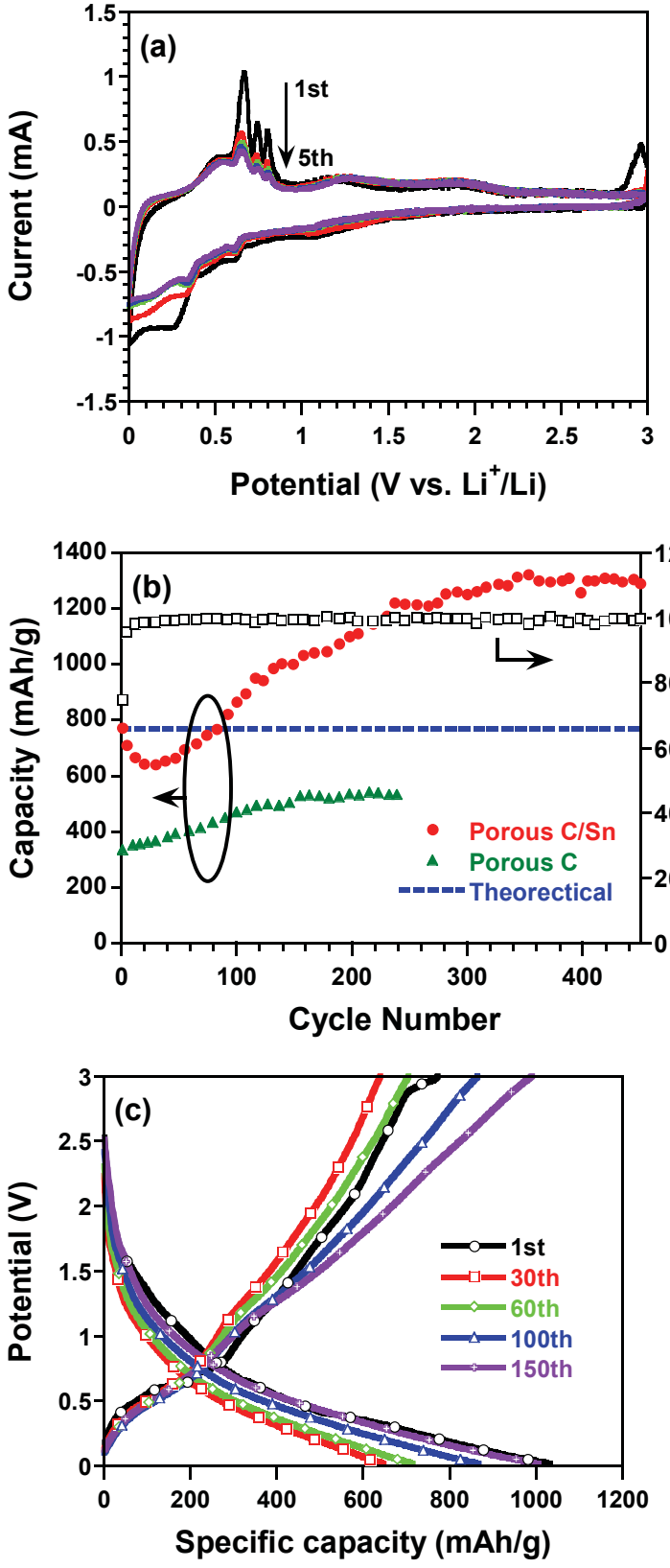

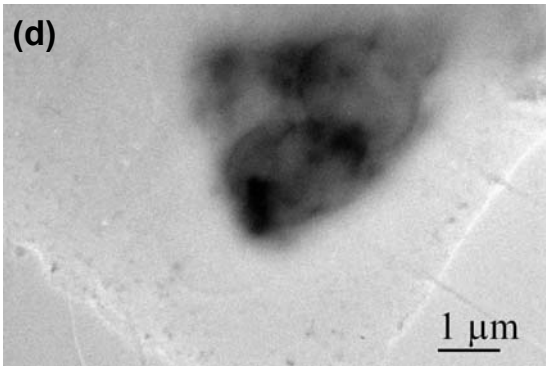

Fig. 5 (a) Cyclic voltammograms of initial 5 cycles of the porous C/Sn. (b) Cycling performance of the porous C/Sn composite (red circle), porous carbon without tin nanoparticles (green triangle) and the theoretical capacity of the porous C/Sn composite based on the capacity of pure porous carbon and the theoretical capacity of metallic tin (blue dashed line). (c) Charge/Discharge profiles at the 1st, 30th, and 100th, and 150th cycle. (d) TEM image of porous C/Sn anode charged to 1 V.

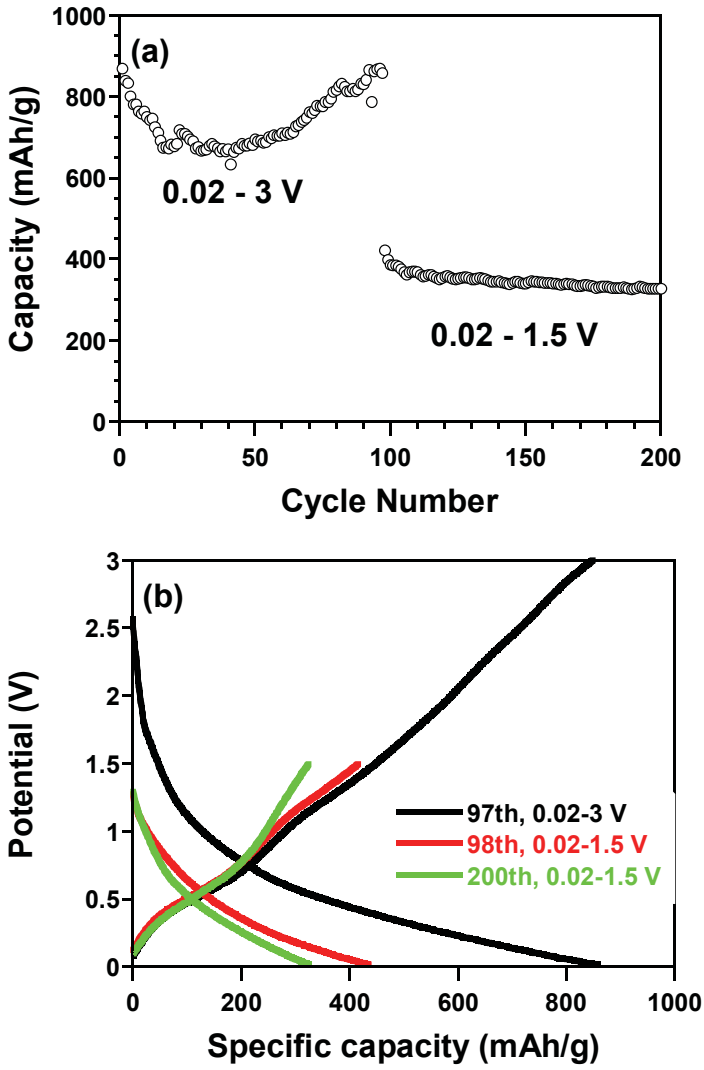

Fig. 6 (a) Cycling performance of the porous C/Sn composite cycled at 0.02 – 3 V and 0.02 – 1.5 V. (b) Charge/discharge curves at 0.02 – 3 V and 0.02 – 1.5V.

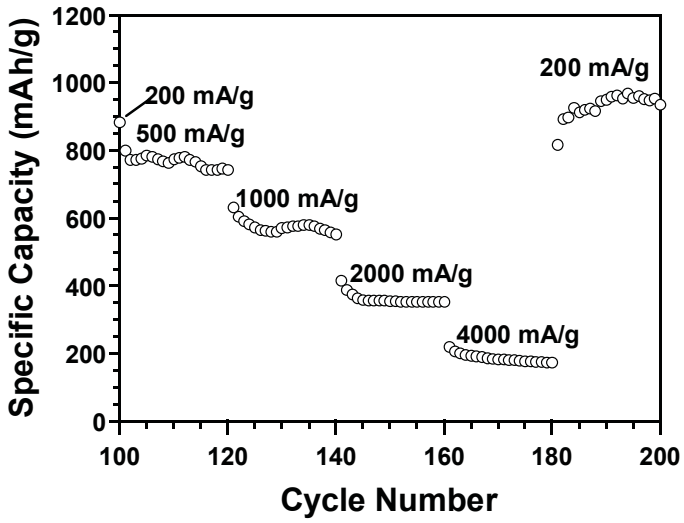

Fig. 7 Rate capability of the porous C/Sn composite at different current densities and 0.02 – 3 V after 100 cycles at 200 mA/g.

TOC Graphical abstract

Mesoporous C/Sn anodes with exceptional capacity and cycling stability are synthesized by dispersing SnO_2 nanoparticles into polymer followed by carbonization.